Inorg. Chem. **2009**, *48*, 2001−2009

Investigating Metal Size Effects in the $Ln_2(\mu\text{-}\eta^2\text{:}\eta^2\text{-}N_2)$ Reduction System: Reductive Reactivity with Complexes of the Largest and Smallest Trivalent Lanthanide Ions, La^{3+} and Lu^{3+}

William J. Evans,* Sara E. Lorenz, and Joseph W. Ziller

Department of Chemistry, University of California, Irvine, California 92697-2025

Received September 28, 2008

Metal size effects in reductive chemistry using $[(C_5Me_4H)_2Ln(THF)]_2(\mu\text{-}\eta^2\text{:}\eta^2\text{-}N_2)$ complexes have been evaluated using the extremes in ionic radii of the lanthanide series, Ln = La, **1**, and Lu, **2**. Comparisons have been made using 1,3,5,7-cyclooctatetraene, phenazine, carbon dioxide, and anthracene as substrates. Complexes **1** and **2** react similarly with 1,3,5,7-cyclooctatetraene to form $(C_5Me_4H)_3Ln$ and $(C_5Me_4H)Ln(C_8H_8)(THF)_x$ (Ln = La, $x = 2$, or Lu, $x = 0$) in a reaction analogous to the reduction of this substrate with divalent $(C_5Me_5)_2Sm$. Complexes **1** and **2** differ in their reactions with phenazine in that **1** forms at least three products, including $[(C_5Me_4H)_2La](\mu\text{-}\eta^4\text{:}\eta^2\text{-}C_{12}H_8N_2)[La(THF)(C_5Me_4H)_2]$, **3**, and $(C_5Me_4H)_3La$, whereas **2** forms a single product, $[(C_5Me_4H)_2Lu]_2(\mu\text{-}\eta^3\text{:}\eta^3\text{-}C_{12}H_8N_2)$, **4**, in quantitative yield. Complexes **3** and **4** are similar to the product obtained from the reaction of $(C_5Me_5)_2Sm$ and phenazine, $[(C_5Me_5)_2Sm]_2(\mu\text{-}\eta^3\text{:}\eta^3\text{-}C_{12}H_8N_2)$, since all three complexes contain a reduced phenazine dianion, but the phenazine ligand displays structural variations depending on the size of the metal. With CO_2, complex **1** forms multiple products, but **2** reacts cleanly to form the reductively coupled oxalate complex, $[(C_5Me_4H)_2Lu]_2(\mu\text{-}\eta^2\text{:}\eta^2\text{-}C_2O_4)$, **5**, in high yield. With anthracene, **1** forms a complex product mixture from which only $(C_5Me_4H)_3La(THF)$, **9**, characterized by X-ray crystallography, could be identified. In contrast, **2** is unreactive toward anthracene even upon heating to 75 °C after 24 h.

Introduction

Molecular divalent lanthanide reduction chemistry has progressed rapidly in recent years.[1−4] After decades of focus on just three ions, Eu^{2+}, Yb^{2+}, and Sm^{2+}, three more elements were found to form molecular complexes of divalent ions that could be used for reduction chemistry in solution, Tm^{2+},[5] Dy^{2+},[6] and Nd^{2+}.[7] In efforts to find easier routes to the reaction chemistry of these divalent ions, it was discovered that the combination of an alkali metal and a trivalent lanthanide complex[8−10] could also provide access to divalent-like reduction chemistry. This so-called LnZ_3/M reaction, Scheme 1, in which Z is an amide or cyclopentadienyl ligand and M is an alkali metal, proved to be a general synthetic method viable for trivalent lanthanides from La to Lu.[11−14] This meant that divalent-like "LnZ_2" chemistry was accessible via Scheme 1, even with the lanthanides for which soluble, molecular, divalent species have never been identified. Access to these virtual divalent oxidation state species is also possible from heteroleptic precursors, that is, LnZ_2Z'/M,[12−14] and can provide analogous "LnZ_2" reactivity.

* To whom correspondence should be addressed. Fax: 949-824-2210. E-mail: wevans@uci.edu.

(1) Bochkarev, M. N. *Coord. Chem. Rev.* **2004**, *248*, 835.
(2) Evans, W. J. *J. Organomet. Chem.* **2002**, *652*, 61.
(3) Evans, W. J. *J. Organomet. Chem.* **2002**, *647*, 2.
(4) Evans, W. J. *Coord. Chem. Rev.* **2000**, *206*, 263.
(5) Bochkarev, M. N.; Fedushkin, I. L.; Fagin, A. A.; Petrovskaya, T. V.; Ziller, J. W.; Broomhall-Dillard, R. N. R.; Evans, W. J. *Angew. Chem., Int. Ed. Engl.* **1997**, *36*, 113.
(6) Evans, W. J.; Allen, N. T.; Ziller, J. W. *J. Am. Chem. Soc.* **2000**, *122*, 11749.
(7) Bochkarev, M. N.; Fedushkin, I. L.; Fagin, A. A.; Dechert, S.; Schumann, H. *Angew. Chem., Int. Ed.* **2001**, *40*, 3176.
(8) Gun'ko, Y. K.; Hitchcock, P. B.; Lappert, M. F. *J. Organomet. Chem.* **1995**, *499*, 213.
(9) Cassani, M. C.; Gun'ko, Y. K.; Hitchcock, P. B.; Lappert, M. F. *Chem. Commun.* **1996**, 1987.
(10) Cassani, M. C.; Gun'ko, Y. K.; Hitchcock, P. B.; Lappert, M. F.; Laschi, F. *Organometallics* **1999**, *18*, 5539.
(11) Evans, W. J.; Lee, D. S.; Rego, D. B.; Perotti, J. M.; Kozimor, S. A.; Moore, E. K.; Ziller, J. W. *J. Am. Chem. Soc.* **2004**, *126*, 14574.
(12) Evans, W. J.; Lee, D. S.; Lie, C.; Ziller, J. W. *Angew. Chem., Int. Ed.* **2004**, *43*, 5517.
(13) Evans, W. J.; Lee, D. S.; Johnston, M. A.; Ziller, J. W. *Organometallics* **2005**, *24*, 6393.
(14) Evans, W. J.; Rego, D. B.; Ziller, J. W. *Inorg. Chem.* **2006**, *45*, 10790.

10.1021/ic801853d CCC: $40.75
Published on Web 01/28/2009

Scheme 1

$$2LnZ_3 + 2M + \text{substrate} \longrightarrow [Z_2Ln]_2(\text{substrate}) + 2MZ$$

$$\text{substrate} + 2e^{1-} \longrightarrow (\text{substrate})^{2-}$$

$$2LnZ_3 + 2M \xrightarrow[-2MZ]{} \text{"}2LnZ_2\text{"} \longrightarrow 2[Z_2Ln]^{1+} + 2e^{1-}$$

Scheme 2

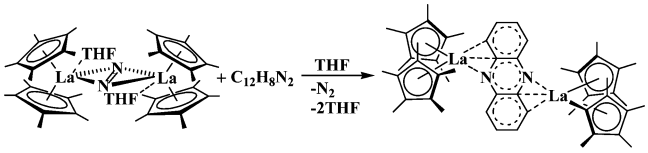

$$C_{12}H_8N_2 + 2e^{1-} \longrightarrow (C_{12}H_8N_2)^{2-}$$

$$(N_2)^{2-} \longrightarrow N_2 + 2e^{1-}$$

These new reductive options provided access to a much wider range of lanthanide dinitrogen complexes, $[Z_2Ln(THF)]_2(\mu\text{-}\eta^2\text{:}\eta^2\text{-}N_2)$, where Z was typically (C_5Me_4R) (R = Me or H) or $[N(SiMe_3)_2]$. Subsequently, it was discovered that $[(C_5Me_5)_2La(THF)]_2(\mu\text{-}\eta^2\text{:}\eta^2\text{-}N_2)$ was also capable of delivering "LnZ_2" reactivity via a $(N_2)^{2-}/N_2$ redox couple.[15] An example with phenazine is shown in Scheme 2.

The $Ln_2(\mu\text{-}\eta^2\text{:}\eta^2\text{-}N_2)$ reductive method provides a unique opportunity to evaluate "LnZ_2"-like reactivity as a function of the size of the lanthanide. In trivalent lanthanide chemistry, the optimization of reactivity based on the radial size of the metal is quite powerful.[16−22] Traditionally, in reactions involving divalent lanthanides, this size optimization was not possible since only a few molecular divalent ions were accessible in solution and did not span the full range of the lanthanide series. Since the $Ln_2(\mu\text{-}\eta^2\text{:}\eta^2\text{-}N_2)$ method of accessing divalent-like chemistry is based on trivalent metal complexes, optimization of reductive reactivity is now possible on the basis of metal size.

It is also possible to examine size optimization of "LnZ_2" reduction chemistry with the LnZ_3/M and LnZ_2Z'/M methods, but because reactive intermediates may be involved that depend on the reduction potentials of the metals, the comparison based on size is more complicated. Since the $Ln_2(\mu\text{-}\eta^2\text{:}\eta^2\text{-}N_2)$ system has a fully defined single molecular component as the reagent, evaluation of size effects can be made more directly.

In this paper, we examine the extremes in size in the lanthanide series, lanthanum and lutetium, in comparative reduction reactions effected by the $Ln_2(\mu\text{-}\eta^2\text{:}\eta^2\text{-}N_2)$ unit. The $(C_5Me_4H)^-$ based complexes, $[(C_5Me_4H)_2La(THF)]_2(\mu\text{-}\eta^2\text{:}\eta^2\text{-}N_2)$, **1**, and $[(C_5Me_4H)_2Lu(THF)]_2(\mu\text{-}\eta^2\text{:}\eta^2\text{-}N_2)$, **2**, were selected since both can be synthesized in good yield and are diamagnetic. For the general reaction shown in eq 1, the effect of metal size on the reductive reactivity is described for both easily reduced substrates such as phenazine as well as more challenging redox targets such as carbon dioxide.

$$[(C_5Me_4H)_2Ln(THF)]_2N_2 + \text{substrate} \xrightarrow[-2THF]{-N_2} [(C_5Me_4H)_2Ln]_2(\text{substrate dianion}) \quad (1)$$

Experimental Section

The manipulations described below were performed under nitrogen or argon with rigorous exclusion of air and water using Schlenk, vacuum line, and glovebox techniques. Solvents were saturated with UHP-grade argon (Airgas) and dried over columns containing Q-5 and molecular sieves. NMR solvents were dried over a NaK alloy and vacuum transferred before use. ^1H and ^{13}C NMR spectra were recorded with a Bruker DRX GN500 MHz system. Infrared spectra were recorded as thin films obtained from benzene-d_6 on the silicon window of the probe of an ASI ReactIR 1000 instrument[23] or as KBr pellets on a PerkinElmer Spectrum One FT-IR spectrometer. $[(C_5Me_4H)_2La(THF)]_2(\mu\text{-}\eta^2\text{:}\eta^2\text{-}N_2)$,[12] **1**, and $[(C_5Me_4H)_2Lu(THF)]_2(\mu\text{-}\eta^2\text{:}\eta^2\text{-}N_2)$,[13] **2**, were prepared as previously described. CO_2 was purchased from Airgas and used as received.[13]CO_2 was purchased from Aldrich and used as received. Phenazine (Aldrich) and anthracene (Aldrich) were purified by sublimation prior to use. 1,3,5,7-Cyclooctatetraene (Aldrich) was distilled over 4 Å molecular sieves and degassed by three freeze−pump−thaw cycles. Elemental analyses were performed by Analytische Laboratorien (Lindlar, Germany) or on a PerkinElmer Series II 2400 CHN elemental analyzer.

1,3,5,7-Cyclooctatetraene Reactions. C_8H_8 (1.7 μL, 0.015 mmol) was added to a NMR tube containing **1** (15 mg, 0.015 mmol) in 1 mL of benzene-d_6. The solution immediately changed from bright yellow to pale yellow. ^1H NMR spectroscopy showed complete consumption of the starting material and formation of the previously characterized complexes, $(C_5Me_4H)La(C_8H_8)(THF)_2$[24] and $(C_5Me_4H)_3La$.[20] This reaction was also performed as described above in THF-d_8 in order to characterize $(C_5Me_4H)La(C_8H_8)(THF)_2$, which has limited solubility in benzene-d_6.

Similarly, C_8H_8 (1.1 μL, 0.010 mmol) was added to a NMR tube containing **2** (9.7 mg, 0.010 mmol) in 1 mL of benzene-d_6. Although no change in the color of the solution was observed, ^1H NMR spectroscopy showed complete consumption of the starting material and formation of the previously characterized complexes, $(C_5Me_4H)Lu(C_8H_8)$[24] and $(C_5Me_4H)_3Lu$.[13]

Phenazine Reactions. $[(C_5Me_4H)_2La](\mu\text{-}\eta^4\text{:}\eta^2\text{-}C_{12}H_8N_2)[La(THF)(C_5Me_4H)_2]$, 3. A yellow solution of **1** (121 mg, 0.12 mmol) in 10 mL of toluene was added to a vial containing phenazine, $C_{12}H_8N_2$ (22 mg, 0.12 mmol). A dark red solution immediately formed. After the mixture was stirred for 30 min, the solution was evaporated to dryness to yield a dark red oily residue. The residue was triturated with hexanes and evaporated to dryness to yield a dark red microcrystalline solid (119 mg). Crystals of **3** suitable for X-ray analysis were grown from a concentrated 1:1 toluene/hexane solution of the isolated

(15) Evans, W. J.; Lee, D. S.; Ziller, J. W.; Kaltsoyannis, N. *J. Am. Chem. Soc.* **2006**, *128*, 14176.
(16) Schumann, H.; Meese-Marktscheffel, J. A.; Esser, L. *Chem. Rev.* **1995**, *95*, 865.
(17) Evans, W. J.; Dominguez, R.; Hanusa, T. P. *Organometallics* **1986**, *5*, 263.
(18) Alvarez, D.; Caulton, K. G.; Evans, W. J.; Ziller, J. W. *J. Am. Chem. Soc.* **1990**, *112*, 5674.
(19) Jeske, G.; Lauke, H.; Mauermann, H.; Schumann, H.; Marks, T. J. *J. Am. Chem. Soc.* **1985**, *107*, 8111.
(20) Schumann, H.; Glanz, M.; Hemling, H. *J. Organomet. Chem.* **1993**, *445*, C1.
(21) Evans, W. J.; Nyce, G. W.; Clark, R. D.; Doedens, R. J.; Ziller, J. W. *Angew. Chem., Int. Ed.* **1999**, *38*, 1801.
(22) Evans, W. J.; Davis, B. L.; Champagne, T. M.; Ziller, J. W. *Proc. Natl. Acad. Sci. U. S. A.* **2006**, *103*, 12678.
(23) Evans, W. J.; Johnston, M. A.; Ziller, J. W. *Inorg. Chem.* **2000**, *39*, 3421.
(24) Schumann, H.; Glanz, M.; Winterfeld, J.; Hemling, H. *J. Organomet. Chem.* **1993**, *456*, 77.

microcrystalline material at −35 °C over the course of two days. The ^{1}H NMR spectrum in benzene-d_6 of the crystalline solid isolated from the reaction displayed three resonances at 5.74, 5.90, and 5.96 ppm (5:5:2 ratio) in the $(C_5Me_4H)^-$ region. The resonance in the ^{1}H NMR at 5.74 ppm is consistent with that of the previously reported complex, $(C_5Me_4H)_3La$,[20] while the resonance at 5.90 ppm can be assigned to **3**, on the basis of integrations. A variable-temperature ^{1}H NMR study in a sealed J-Young NMR tube in toluene-d_8 over a temperature range of 298 to 393 K did not lead to a simplification of the spectrum and did not provide evidence of a monomer/dimer equilibrium. Elemental analysis of the crystalline material did not match the composition of **3** but, instead, was more consistent with the formation of a mono(cyclopentadienyl) product, $(C_5Me_4H)La(C_{12}H_8N_2)(THF)$. ^{1}H NMR (benzene-$d_6$): δ 1.85 (s, C_5Me_4H, 15H), 1.97 (s, C_5Me_4H, 6H), 2.02 (s, C_5Me_4H, 15H), 2.05 (s, C_5Me_4H, 16H), 2.14 (s, C_5Me_4H, 6H), 2.16 (s, C_5Me_4H, 16H), 5.46 (m, $C_{12}H_8N_2$, 2.5H), 5.68 (d, $C_{12}H_8N_2$, 1H), 5.74 (s, C_5Me_4H, 2.5H), 5.90 (s, C_5Me_4H, 2.5H), 5.94 (d, $C_{12}H_8N_2$, 1H), 5.96 (s, C_5Me_4H, 1H), 6.27 (m, $C_{12}H_8N_2$, 2.5H), 6.41 (t, $C_{12}H_8N_2$, 1H), 6.50 (t, $C_{12}H_8N_2$, 1H).

$[(C_5Me_4H)_2Lu]_2(\mu\text{-}\eta^3\text{:}\eta^3\text{-}C_{12}H_8N_2)$, 4. A yellow solution of **2** (182 mg, 0.18 mmol) in 10 mL of toluene was added to a vial containing phenazine (33 mg, 0.18 mmol). A dark red solution immediately formed. After the mixture was stirred for 30 min, the solution was evaporated to dryness to yield a dark red oily residue. The residue was triturated with hexanes and evaporated to dryness to yield a dark red microcrystalline solid (199 mg, 99%). Crystals of **4** suitable for X-ray analysis were grown from a concentrated 1:1 toluene/hexane solution at −35 °C over the course of two days. ^{1}H NMR (benzene-d_6): δ 2.04 (s, $C_5\mathit{Me}_4H$, 24H), 2.20 (s, $C_5\mathit{Me}_4H$, 24H), 5.01 (m, $C_{12}\mathit{H}_8N_2$, 4H), 6.01 (m, $C_{12}\mathit{H}_8N_2$, 4H), 6.03 (s, $C_5Me_4\mathit{H}$, 4H). ^{13}C NMR (126 MHz, benzene-d_6): δ 146.81 ($\mathit{C}_8H_{12}N_2$), 122.54 (C_5Me_4H), 121.92 ($\mathit{C}_8H_{12}N_2$), 118.09 (C_5Me_4H), 112.31 (C_5Me_4H), 103.68 ($\mathit{C}_8H_{12}N_2$), 12.94 ($C_5\mathit{Me}_4H$), 11.08 ($C_5\mathit{Me}_4H$). IR: 2910s, 2860s, 1513w, 1436w, 1382w, 1328w, 1301w, 1262s, 1077s, 1019s, 799s, 749s, 656s cm^{-1}. Anal. calcd for $C_{48}H_{60}Lu_2N_2$: C, 56.80; H, 5.96; N, 2.76. Found: C, 55.97; H, 6.39; N, 2.65.

CO_2 Reaction. $[(C_5Me_4H)_2Lu]_2(\mu\text{-}\eta^2\text{:}\eta^2\text{-}C_2O_4)$, 5. A sealable Schlenk flask was charged with **2** (205 mg, 0.20 mmol) in 25 mL of benzene. Since **2** is not entirely soluble in benzene, THF (1 mL) was added to the yellow suspension to form a yellow solution. The Schlenk flask was attached to a high-vacuum line, and the solution was degassed by three freeze−pump−thaw cycles. Carbon dioxide at 1 atm was introduced into the system. The bright yellow solution turned pale yellow within 5 min of the addition of the CO_2. After the solution was stirred for 3 h, the solution was evaporated to dryness to yield a pale yellow powder (180 mg, 95%). Crystals of **5** suitable for X-ray analysis were grown from a concentrated benzene/THF (25:1) solution at −35 °C overnight. ^{1}H NMR (benzene-d_6): δ 1.95 (s, $C_5\mathit{Me}_4H$, 24H), 1.97 (s, $C_5\mathit{Me}_4H$, 24H), 5.87 (s, $C_5Me_5\mathit{H}$, 4H). ^{13}C NMR (126 MHz, benzene-d_6): δ 168.51 (C_2O_4), 120.14 (C_5Me_4H), 117.28 (C_5Me_4H), 111.06 (C_5Me_4H), 12.34 ($C_5\mathit{Me}_4H$), 11.01 ($C_5\mathit{Me}_4H$). IR: 2964m, 2910m, 2860m, 1656s, 1567s, 1505s, 1417s, 1309m, 1262s, 1189w, 1092s, 1023s, 799s cm^{-1}. Anal. calcd for $C_{38}H_{52}Lu_2O_4$: C, 48.01; H, 5.56. Found: C, 49.46; H, 5.68. ^{13}C-labeled **5**-$^{13}\mathit{C}_2O_4$ was synthesized in an analogous fashion using $^{13}CO_2$.

Anthracene Reactions. A yellow solution of **1** (105 mg, 0.109 mmol) in 10 mL of toluene was added to a vial containing anthracene (19.4 mg, 0.109 mmol). The solution immediately turned dark green. The solution was allowed to stir overnight and was evaporated to dryness to yield a dark green oily residue. The residue was triturated with hexanes and evaporated to dryness to yield a dark green microcrystalline solid (102 mg). Crystals of $(C_5Me_4H)_3La(THF)$, **9**, suitable for X-ray analysis were grown from a concentrated toluene solution of the isolated microcrystalline material at −35 °C overnight. The ^{1}H NMR spectrum, in benzene-d_6, of the crystalline solid isolated from the reaction displayed two resonances at 5.74 and 5.79 ppm in the $(C_5Me_4\mathit{H})^-$ region in a 12:1 ratio. The resonance at 5.74 ppm matches that of $(C_5Me_4H)_3La$.[20]

X-Ray Data Collection, Structure Solution, and Refinement of 3. A red crystal of approximate dimensions 0.04 × 0.17 × 0.25 mm was mounted on a glass fiber and transferred to a Bruker CCD platform diffractometer. The SMART[25] program package was used to determine the unit-cell parameters and for data collection (30 s/frame scan time for a sphere of diffraction data). The raw frame data was processed using SAINT[26] and SADABS[27] to yield the reflection data file. Subsequent calculations were carried out using the SHELXTL[28] program. The diffraction symmetry was 2/*m*, and the systematic absences were consistent with the centrosymmetric monoclinic space group $P2_1/n$ that was later determined to be correct. The structure was solved by direct methods and refined on F^2 by full-matrix least-squares techniques. The analytical scattering factors[29] for neutral atoms were used throughout the analysis. Hydrogen atoms were included using a riding model.

X-Ray Data Collection, Structure Solution, and Refinement of 4. A red crystal of approximate dimensions 0.055 × 0.24 × 0.29 mm was handled as described above. Data was collected using a 25 s/frame scan time. The diffraction symmetry was 2/*m*, and the systematic absences were consistent with the monoclinic space groups *Cc* and *C*2/*c*. It was later determined that the centrosymmetric space group *C*2/*c* was correct.

X-Ray Data Collection, Structure Solution, and Refinement of 5. A yellow crystal of approximate dimensions 0.10 × 0.15 × 0.25 mm was handled as described for **3**. Data was collected using a 25 s/frame scan time. Due to crystal cracking, it was necessary to collect the diffraction data at 263 K. The diffraction symmetry was 2/*m*, and the systematic absences were consistent with the centrosymmetric monoclinic space group $P2_1/n$ that was later determined to be correct. The molecule is located about an inversion center. The tetramethylcyclopentadienyl ligand defined by atoms C(10)−C(19) was disordered. Carbon atoms C(16), C(17), and C(19) and their associated hydrogen atoms were included with partial site-occupancy factors of 0.725, 0.725, and 0.550, respectively. The aromatic hydrogen atom was not located or included in the refinement.

X-Ray Data Collection, Structure Solution, and Refinement of 9. A green crystal of approximate dimensions 0.25 × 0.25 × 0.26 mm was mounted on a glass fiber and transferred to a Bruker SMART APEX II diffractometer. The APEX 2[30] program package was used to determine the unit-cell parameters and for data collection (15 s/frame scan time for a sphere of diffraction data). The raw frame data were processed using SAINT[31] and SADABS[32] to yield the reflection data file. Subsequent calculations were carried

(25) *SMART Software Users Guide*, version 5.1; Bruker Analytical X-raySystems, Inc.: Madison, WI, 1999.
(26) *SAINT Software Users Guide*, version 6.0; Bruker Analytical X-raySystems, Inc.: Madison, WI, 1999.
(27) Sheldrick, G. M. *SADABS*, version 2.10; Bruker Analytical X-raySystems, Inc.: Madison, WI, 2002.
(28) Sheldrick, G. M. *SHETLXTL*, version 6.12; Bruker Analytical X-raySystems, Inc.: Madison, WI, 2001.
(29) *International Tables for X-Ray Crystallography*; Kluwer Academic Publishers: Dordrecht, The Netherlands, 1992; Vol. C.
(30) *APEX*, version 2008.3-0; Bruker AXS, Inc.: Madison, WI, 2007.
(31) *SAINT*, version 7.53a; Bruker AXS, Inc.: Madison, WI, 2007.

out using the SHELXTL[28] program. The systematic absences were consistent with the cubic space group $Pa\bar{3}$ that was assigned and later determined to be correct.

The structure was solved using the coordinates of the uranium analogue and refined on F^2 by full-matrix least-squares techniques. The analytical scattering factors[29] for neutral atoms were used throughout the analysis. The molecule was located on a 3-fold rotation axis, resulting in disorder of the THF ligand. Carbon atoms C(10), C(11), and C(12) were included with partial site-occupancy factors and isotropic thermal parameters. Hydrogen atoms associated with the disordered THF were not included in the refinement. The remaining hydrogen atoms were included using a riding model.

Results

1,3,5,7-Cyclooctatetraene Reactivity. Complexes **1** and **2** react similarly with 1,3,5,7-cyclooctatetraene, C_8H_8, which has reported reduction potentials of −1.62 to −1.86 V versus SCE.[33] In each case, complete consumption of the starting material occurs, and the corresponding complexes, $(C_5Me_4H)Ln(C_8H_8)(THF)_x$[24] and $(C_5Me_4H)_3Ln$,[13,20] are formed according to eq 2. Both the lanthanum- and lutetium-containing products in eq 2 had been previously characterized[13,20,24] so that identification could be made by ^{1}H NMR spectroscopy.

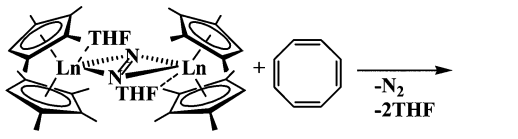

(Ln = La, **1**; Lu, **2**) **(2)**

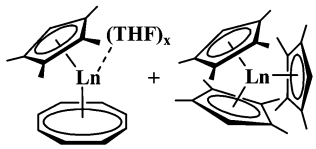

(Ln = La, x = 2; Lu, x = 0)

Equation 2 is analogous to the reaction of 2 equiv of the divalent complex $(C_5Me_5)_2Sm$ with C_8H_8,[34] as shown in eq 3. Similar reactivity has also been observed between 1,3,5,7-cyclooctatetraene and the $(C_5Me_5)^-$ substituted analog of complex **1**, $[(C_5Me_5)_2La(THF)]_2(\mu\text{-}\eta^2\text{:}\eta^2\text{-}N_2)$,[15] to produce $(C_5Me_5)La(C_8H_8)$[35] and $(C_5Me_5)_3La$.[36] Equation 2 demonstrated that $[(C_5Me_4H)_2Ln]_2(\mu\text{-}\eta^2\text{:}\eta^2\text{-}N_2)$ reductive reactivity equivalent to that of divalent Ln^{2+} complexes was accessible for both **1** and **2**. In contrast to eq 2, the reactions discussed below reveal just how varied the reactivity of **1** and **2** can be.

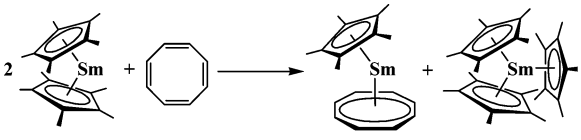

(3)

Phenazine Reactivity. Complexes **1** and **2** both react immediately with phenazine (−0.364 V vs SCE)[37] to form dark red solutions. Each reaction produced crystals of a bimetallic reduced phenazine complex similar to the product shown in Scheme 2. These complexes, $[(C_5Me_4H)_2La](\mu\text{-}\eta^4\text{:}\eta^2\text{-}C_{12}H_8N_2)[La(THF)(C_5Me_4H)_2]$, **3**, and $[(C_5Me_4H)_2Lu]_2(\mu\text{-}\eta^3\text{:}\eta^3\text{-}C_{12}H_8N_2)$, **4**, were isolated and characterized by X-ray crystallography, Figures 1 and 2.

Complex **4**, was isolated in quantitative yield according to eq 4 and was completely characterized by IR, ^{1}H, and ^{13}C NMR spectroscopy. This reaction is analogous to the reaction of $(C_5Me_5)_2Sm$ with phenazine to form $[(C_5Me_5)_2Sm]_2(\mu\text{-}\eta^3\text{:}\eta^3\text{-}C_{12}H_8N_2)$, **6**, shown in eq 5.[34]

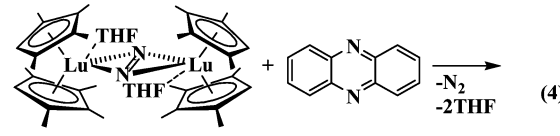

(4)

2

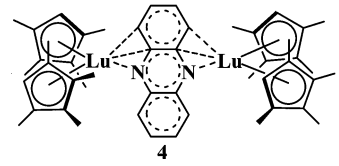

4

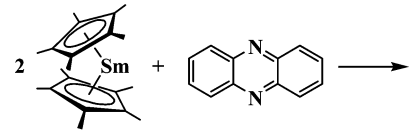

(5)

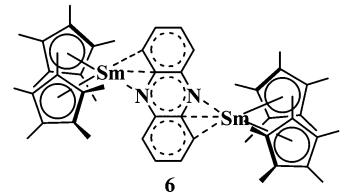

6

In contrast, the reaction of **1** with phenazine to form **3** was more complicated. The ^{1}H NMR spectrum of the *crystals* isolated from the reaction of **1** with phenazine displayed multiple resonances in the $(C_5Me_4H)^-$ region, including resonances consistent with the formation of $(C_5Me_4H)_3La$,[20] which was subsequently identified by X-ray crystallography. The formation of $(C_5Me_4H)_3La$ in this reaction makes this lanthanum reaction similar to the reductions that occur in eqs 2 and 3. $(C_5Me_4H)_3La$ could form via ligand redistribution of complex **3**, as shown in eq 6, although the expected monocyclopentadienyl byproduct, $(C_5Me_4H)La(C_{12}H_8N_2)(THF)_x$, was not definitively identified.

CO_2 Reactivity. Neither **1** nor **2** react with naphthalene, which has a reported reduction potential of −2.60 V versus SCE.[37] However, reactivity is observed with CO_2, for which reduction potentials as negative as −2.21 V versus SCE have been reported in dimethylformamide.[38] Complex **1** reacts

(32) Sheldrick, G. M. *SADABS*, version 2007/4; Bruker AXS, Inc.: Madison, WI, 2007.
(33) Mann, C. K.; Barnes, K. K. *Electrochemical Reactions in Nonaqueous Systems*; Bard, A. J., Ed.; Marcel Dekker, Inc.: New York, 1970.
(34) Evans, W. J.; Gonzales, S. L.; Ziller, J. W. *J. Am. Chem. Soc.* **1991**, *113*, 7423.
(35) Schumann, H.; Kohn, R. D.; Reier, F.-W.; Dietrich, A.; Pickardt, J. *Organometallics* **1989**, *8*, 1388.
(36) Evans, W. J.; Davis, B. L.; Ziller, J. W. *Inorg. Chem.* **2001**, *40*, 6341.
(37) de Boer, E. *Adv. Organomet. Chem.* **1964**, *2*, 115.
(38) Lamy, E.; Nadjo, L.; Saveant, J. M. *Electroanal. Chem.* **1977**, *78*, 403.

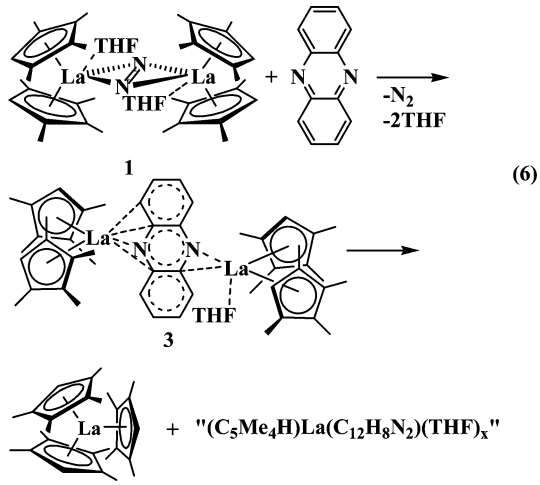

immediately with CO_2 at 1 atm in a benzene/THF solution to form a pale yellow solution. The ^{1}H NMR spectrum showed complete consumption of the starting material and at least 20 distinguishable resonances in the $(C_5Me_4H)^{1-}$ region from 1.64 to 2.57 ppm; no single crystalline product was isolated from this reaction. It has previously been shown that reactions of CO_2 with $(C_5Me_4H)^-$ lanthanide complexes, such as $(C_5Me_4H)_3La$, can be quite complicated due to the insertion of CO_2 into multiple positions in the tetramethylcyclopentadienyl ligand to produce various isomers of the cyclopentadienyl carboxylate, $[C_5Me_4HCO_2]^-$.[39]

In contrast to the reaction of **1** with CO_2, complex **2** reacts cleanly within 5 min to form a yellow compound, $[(C_5Me_4H)_2Lu]_2(\mu\text{-}\eta^2\text{:}\eta^2\text{-}C_2O_4)$, **5**, in 95% yield, eq 7, which is analogous to the reduction of CO_2 by divalent Sm^{2+} metallocenes, eq 8. Complex **5** was characterized by IR, ^{1}H, and ^{13}C NMR spectroscopy and identified by X-ray crystallography, Figure 3. In addition, the synthesis of ^{13}C-labeled **5**, $[(C_5Me_4H)_2Lu]_2(\mu\text{-}\eta^2\text{:}\eta^2\text{-}^{13}C_2O_4)$, using $^{13}CO_2$ was performed in order to identify oxalate absorptions in the IR spectrum. As expected, the absorption at 1656 cm^{-1} in the spectrum of **5**, originally assigned as the ν_{CO} of the oxalate ligand,[40] is absent in the ^{13}C-labeled analog. Increased intensity is observed around 1620 cm^{-1} where the absorption for the ^{13}C-labeled complex would be expected, but multiple absorptions in the 1637−1572 cm^{-1} region preclude exact assignment of the shifted absorption.

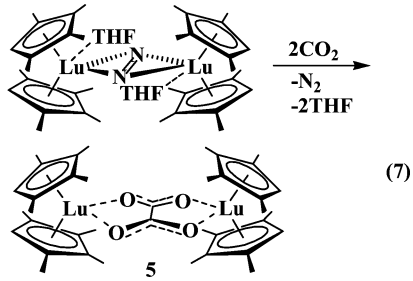

Anthracene Reactivity. There is also a significant difference in the reactivities observed between complexes

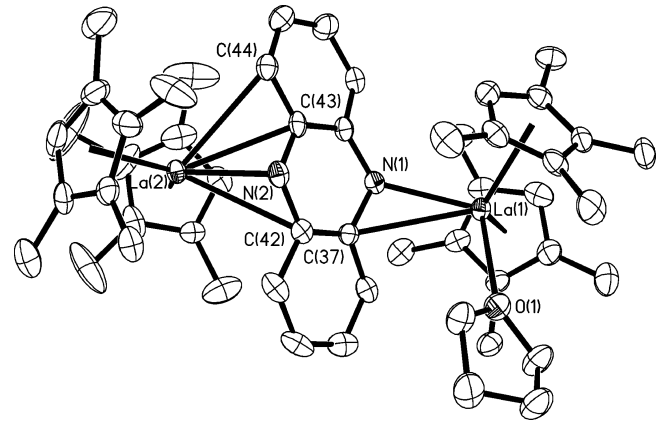

Figure 1. Thermal ellipsoid plot of $[(C_5Me_4H)_2La](\mu\text{-}\eta^4\text{:}\eta^2\text{-}C_{12}H_8N_2)$-$[La(THF)(C_5Me_4H)_2]$, **3**, drawn at the 50% probability level. Hydrogen atoms are omitted for clarity.

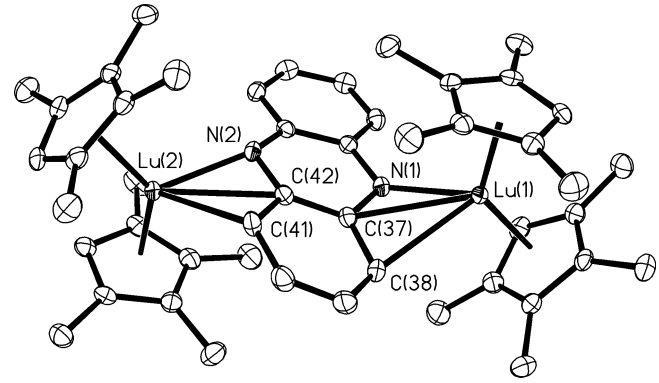

Figure 2. Thermal ellipsoid plot of $[(C_5Me_4H)_2Lu]_2(\mu\text{-}\eta^3\text{:}\eta^3\text{-}C_{12}H_8N_2)$, **4**, drawn at the 50% probability level. Hydrogen atoms are omitted for clarity.

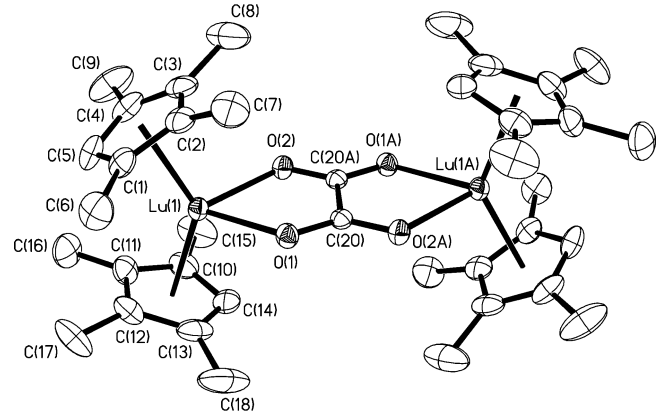

Figure 3. Thermal ellipsoid plot of $[(C_5Me_4H)_2Lu]_2(\mu\text{-}\eta^2\text{:}\eta^2\text{-}C_2O_4)$, **5**, drawn at the 30% probability level. Hydrogen atoms are omitted for clarity. Disorder in the C(10)−C(14) ring where the hydrogen atom of the $(C_5Me_4H)^-$ ligand displays partial site occupancy over C(16), C(17), and C(19) is not shown.

1 and **2** with anthracene, which has reduction potentials of −1.98 and −2.44 V versus SCE.[37] Complex **2** showed no reactivity toward this substrate, even when heated to 75 °C for 24 h. In contrast, the addition of anthracene to complex **1** resulted in an immediate color change from yellow to dark green in benzene-d_6 at room temperature. The ^{1}H NMR spectrum indicated the complete consumption of **1** accompanied by the formation of four resonances in the $(C_5Me_4H)^-$ region and two resonances in the

(39) Evans, W. J.; Rego, D. B.; Ziller, J. W.; DiPasquale, A. G.; Rheingold, A. L. *Organometallics* **2007**, *26*, 4737.
(40) Wang, X.-Z.; Wu, J.-G.; Jin, T.-Z.; Shi, N.; Xu, G.-X. *Mikrochim. Acta* **1988**, *I*, 235.

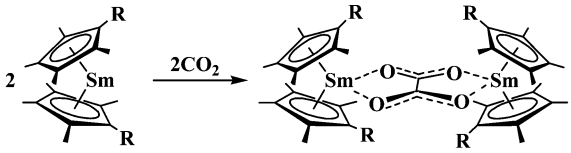

8

R = Me or $SiMe_2CH_2CH=CH_2$, **8**

$(C_5Me_4H)^-$ region consistent with two different $(C_5Me_4H)^-$ environments. The only product that could be definitively identified in the ^1H NMR spectrum of the reaction mixture was $(C_5Me_4H)_3La(THF)$, **9**, which was confirmed by X-ray crystallography, Figure 4.

Structural Discussion. Structures of the Phenazine Products. Complexes **3** and **4** each contain a bridging phenazine dianion, $(C_{12}H_8N_2)^{2-}$, similar to those in $[(C_5Me_5)_2Sm]_2(C_{12}H_8N_2)$,[41] **6**, eq 5, and $[(C_5Me_5)_2La]_2(C_{12}H_8N_2)$,[15,42] **7**, Scheme 2. X-ray data for complexes **3** and **4** are provided in Table 1, while Table 2 compares the metrical data of complexes **3**, **4**, **6**, and **7**.

In each of these complexes, the shortest interaction between the $(C_{12}H_8N_2)^{2-}$ ligand and the metal is through the nitrogen atoms. The 2.472(4) Å La(1)−N(1) and 2.439(4) Å La(2)−N(2) distances in **3** are similar to the analogous 2.452(2) Å La−N distance observed in **7** and are larger than the 2.360(2) Å Sm−N distance observed in **6**, as expected considering that the nine-coordinate ionic radius of La^{3+} is 0.08 Å greater than that of Sm^{3+}.[43] The 2.231(2) Å and 2.248(2) Å Lu−N distances in **4** are smaller, consistent with an 0.18 Å shorter nine-coordinate radius of Lu^{3+} versus La^{3+}.[43]

In addition to the metal nitrogen interactions described above, the metals in **3**, **4**, **6**, and **7** are also oriented toward the carbon atoms adjacent to each nitrogen atom present in the phenazine ring. This contrasts with the structure of $[Mg_2Br_2(C_{12}H_8N_2)(THF)_6]\cdot[MgBr_2(THF)_4]$[44] in which the 2.991−5.467 Å Mg···C distances are significantly larger than the 2.052(7) Å Mg−N bond length.

The structures of **3** and **4** are disparate from each other and from the two similar structures of **6** and **7** in terms of the orientation of the metals to the reduced phenazine dianion. In complexes **6** and **7**, each metal appears to be oriented toward two additional carbon atoms in the ring forming a pseudo aza-allyl bonding mode. The Ln−C $(C_{12}H_8N_2)$ distances in complexes **6** and **7** are longer than any other metal ligand interactions in the complex but are within 0.1−0.2 Å of the Ln−C(C_5Me_5) distances, as is typical for long-range agostic interactions in organolanthanide complexes.[45] In addition, the metals in **6** and **7** are located symmetrically at either end of the reduced phenazine ligand such that the agostic interactions of one metal do not involve the same ring as those of the other.

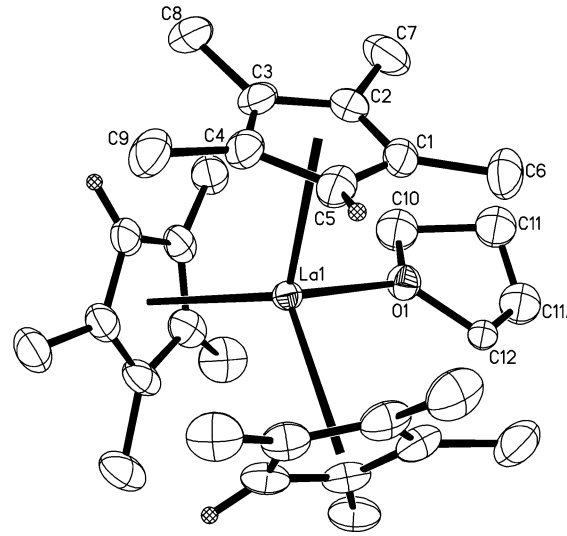

Figure 4. Thermal ellipsoid plot of $(C_5Me_4H)_3La(THF)$, **9**, drawn at the 50% probability level. Complex **9** is located on a 3-fold rotation axis, and the disorder in the THF ligand has been omitted for clarity. Methyl and THF hydrogen atoms are omitted for clarity.

Table 1. X-Ray Data Collection Parameters for Complexes **3**, **4**, **5**, and **9**

	3	**4**	**5**	**9**
empirical formula	$C_{52}H_{68}La_2N_2O$	$C_{48}H_{60}Lu_2N_2$	$C_{38}H_{52}Lu_2O_4$	$C_{31}H_{47}LaO$
fw	1014.90	1014.92	922.74	574.60
temperature (K)	158(2)	163(2)	263(2)	103(2)
cryst syst	monoclinic	monoclinic	monoclinic	cubic
space group	$P2_1/n$	$C2/c$	$P2_1/n$	$Pa\bar{3}$
a (Å)	9.8474(11)	39.835(4)	8.468(9)	17.7403(4)
b (Å)	20.507(2)	9.6073(8)	10.621(11)	17.7403(4)
c (Å)	23.444(3)	26.750(2)	20.19(2)	17.7403(4)
α (deg)	90	90	90	90
β (deg)	92.835(2)	127.2740(10)	97.61(2)	90
γ (deg)	90	90	90	90
volume, Å^3	4728.4(9)	8146.4(12)	1800(3)	5583.2(2)
Z	4	8	2	8
ρ_{calcd} (Mg/m^3)	1.426	1.655	1.703	1.367
μ (mm^{-1})	1.820	4.854	5.489	1.550
R1 [$I > 2.0\sigma(I)$]	0.0373	0.0209	0.0321	0.0447
wR2 (all data)	0.0820	0.0497	0.0811	0.1095

In contrast, the shortest Lu−C$(C_{12}H_8N_2)$ distances in complex **4** involve C(37), C(38), C(41), and C(42), which are all part of the same ring; that is, the metals are at the same end of the reduced phenazine dianion, not at opposite ends as observed for **6** and **7**. Complex **3** is different in that one of the lanthanum metal centers, La(1), coordinates an additional THF molecule of solvation. This leads to an asymmetric binding of the $(C_{12}H_8N_2)^{2-}$ ligand such that only one other atom of the ligand, C(37), is oriented toward La(1) in addition to the La(1)−N(1) linkage. On the other side of the molecule, the La(2) center contains three carbon atoms in the reduced phenazine within 0.2 Å of the La−C(C_5Me_5) distances, C(42) on one side of N(2) and C(43) and C(44) on the other side.

Another difference between the $(C_5Me_4H)^-$-containing complexes, **3** and **4**, and the $(C_5Me_5)^-$-containing complexes, **6** and **7**, is shown in Figure 5. Both **3** and **4** have nonplanar reduced phenazine rings with nitrogen out-of-plane displacements ranging from 0.13 to 0.30 Å. In contrast, the reduced phenazine

(41) Evans, W. J.; Gonzales, S. L.; Ziller, J. W. *J. Am. Chem. Soc.* **1994**, *116*, 2600.
(42) Scholz, J.; Scholz, A.; Weimann, R.; Janiak, C.; Schumann, H. *Angew. Chem., Int. Ed.* **1994**, *33*, 1171.
(43) Shannon, R. D. *Acta Crystallogr.* **1976**, *A32*, 751.
(44) Junk, P. C.; Raston, C. L.; Skelton, B. W.; White, A. H. *Chem. Commun.* **1987**, 1162.
(45) Den Haan, K. H.; de Boer, J. L.; Teuben, J. H. *Organometallics* **1986**, *5*, 1726.
(46) Evans, W. J.; Perotti, J. M.; Brady, J. C.; Ziller, J. W. *J. Am. Chem. Soc.* **2003**, *125*, 5204.

Table 2. Selected Bond Distances (Å) and Angles (deg) for $[(C_5Me_4H)_2La](\mu\text{-}\eta^4\text{:}\eta^2\text{-}C_{12}H_8N_2)[La(THF)(C_5Me_4H)_2]$, **3**; $[(C_5Me_4H)_2Lu]_2(\mu\text{-}\eta^3\text{:}\eta^3\text{-}C_{12}H_8N_2)$, **4**; $[(C_5Me_5)_2Sm]_2(\mu\text{-}\eta^3\text{:}\eta^3\text{-}C_{12}H_8N_2)$,[41] **6**; and $[(C_5Me_5)_2La]_2(\mu\text{-}\eta^3\text{:}\eta^3\text{-}C_{12}H_8N_2)$,[42] **7**

	3 (Ln = La)	**4** (Ln = Lu)	**6** (Ln = Sm)	**7** (Ln = La)
Ln(1)−N(1)	2.472(4)	2.248(2)	2.360(2)	2.452(2)
Ln(2)−N(2)	2.439(4)	2.231(2)		
Ln(1)−C(37)	3.045(5)	2.755(3)		
Ln(1)−C(38)	3.141(5)	2.719(3)		
Ln(1)−C(25)			2.866(3)	
Ln(1)−C(26)			2.877(2)	
Ln(1)−C(21)				2.920(2)
Ln(1)−C(22)				2.931(2)
Ln(2)−C(41)		2.740(3)		
Ln(2)−C(42)	3.089(5)	2.762(3)		
Ln(2)−C(43)	2.867(5)			
Ln(2)−C(44)	3.039(5)			
Ln(1)−Cnt1	2.571	2.301	2.436	2.525
Ln(1)−Cnt2	2.558	2.272	2.421	2.541
Ln(2)−Cnt3	2.525	2.275		
Ln(2)−Cnt4	2.534	2.299		
Cnt1−Ln(1)−Cnt2	125.8	133.5	136.4	135.9
Cnt3−Ln(2)−Cnt4	130.9	133.7		
maximum N (atom) distortion from the phenazine plane	N(1) ± 0.3010	N(1) ± 0.1333	N(1) ± 0.0609	N(1) ± 0.0586
maximum C (atom) distortion from the phenazine plane	C(46) ± 0.2335	C(38) ± 0.1694	C(25) ± 0.0357	C(22) ± 0.0407
Ln−C (C_5Me_4R) range (R = H, **3** and **4**; R = Me, **6** and **7**)	2.761(5)−2.902(5)	2.514(2)−2.641(3)	2.684−2.722	2.783−2.824

Table 3. Selected Bond Distances (Å) and Angles (deg) for $[(C_5Me_4H)_2Lu]_2(\mu\text{-}\eta^2\text{:}\eta^2\text{-}C_2O_4)$, **5**, and $\{[(C_5Me_4)SiMe_2(CH_2CH{=}CH_2)]_2Sm\}_2(\mu\text{-}\eta^2\text{:}\eta^2\text{-}C_2O_4)$,[46] **8**

	5 (Ln = Lu)	**8** (Ln = Sm)
Ln(1)−O(1)	2.242(4)	2.400(2)
Ln(1)−O(2)	2.238(4)	2.398(2)
Ln(1)−Cnt1	2.272	2.445
Ln(1)−Cnt2	2.274	2.426
Cnt1−Ln(1)−Cnt2	135.5	137.1
C(20)−C(20A)	1.551(8)	
C(20)−O(1)	1.255(5)	
C(20)−O(2′)	1.252(5)	
C(20′)−O(1′)	1.255(5)	
C(20′)−O(2)	1.252(5)	
C(29)−C(29′)		1.560(6)
C(29′)−O(2′)		1.253(4)
C(29′)−O(1′)		1.257(4)
C(29)−O(2)		1.253(4)
C(29)−O(1)		1.257(4)

rings in **6** and **7** are planar within 0.06 Å. Figure 5 shows the subtle differences in the ring structure of the $(C_{12}H_8N_2)^{2-}$ ligand as a function of metal size and ligand environment.

Structure of $[(C_5Me_4H)_2Lu]_2(\mu\text{-}\eta^2\text{:}\eta^2\text{-}C_2O_4)$, 5. Complex **5** can be compared to the analogous oxalate complex, $\{[(C_5Me_4)SiMe_2(CH_2CH{=}CH_2)]_2Sm\}_2(\mu\text{-}\eta^2\text{:}\eta^2\text{-}C_2O_4)$,[46] **8**, obtained as shown in eq 8 (R = $SiMe_2CH_2CH{=}CH_2$). Although the $(C_5Me_5)^-$-containing analog of the oxalate complex, $[(C_5Me_5)_2Sm]_2(\mu\text{-}\eta^2\text{:}\eta^2\text{-}C_2O_4)$,[47] has also been prepared, eq 8 (R = Me), the data were of limited quality, and only the connectivity could be determined. The metrical data for complexes **5** and **8** are compared in Table 2.

The structures of complexes **5** and **8** are similar. The oxalate binding to each metallocene is essentially identical, and the Ln−O(oxalate) distances are as expected on the basis of ionic radii.[43] The metrical parameters of the oxalate ligands in **5** and **8** are indistinguishable as expected for an oxalate ligand in an ionic metal complex.

Structure of $(C_5Me_4H)_3La(THF)$, 9. Complex **9** can be compared to that of the analogous uranium complex, $(C_5Me_4H)_3U(THF)$,[48] **10**, as well as the unsolvated analog $(C_5Me_4H)_3La$,[20] **11**, Table 4. Both **9**, Figure 4, and **10** display a pseudotetrahedral geometry with 100.3° and 100.4° (C_5Me_4H ring centroid)−M−O(THF) angles and 116.9° and 116.8° (C_5Me_4H ring centroid)−M−(C_5Me_4H ring centroid) angles, respectively. This differs from **11**, which displays a trigonal-planar geometry with 120° (C_5Me_4H ring centroid)−M−(C_5Me_4H ring centroid) angles. The pseudotetrahedral structure of **9**, like **10**, is as expected since the $(C_5Me_4H)^-$ rings must distort from the trigonal arrangement in order to accommodate the THF ligand. As in **10**, the THF ligand in **9** is located on a 3-fold rotation axis and as a result is disordered. The La−(C_5Me_4H ring centroid) distance in **9**, 2.643 Å, is slightly longer than the 2.616 Å distance in the unsolvated **11**, as expected for a higher-coordinate complex. The La−(C_5Me_4H ring centroid) distance in **9** is also larger than the U−(C_5Me_4H ring centroid) in **10**, 2.597 Å, even after the small difference of 0.007 Å between the ionic radii of the metals[42] is taken into account. Hence, it appears that the lanthanide complex **9** displays longer M−(C_5Me_4H ring centroid) distances than the analogous uranium complex **10**. Such differences, when observed in uranium complexes, are often attributed to increased covalency.

Discussion

The results described above with C_8H_8, eq 2, show that the lanthanum and lutetium complexes $[(C_5Me_4H)_2Ln(THF)]_2(\mu\text{-}\eta^2\text{:}\eta^2\text{-}N_2)$, **1** and **2**, respectively, can function as two electron reductants with reactivity analogous to that expected from 2 equiv of a divalent "$(C_5Me_4H)_2Ln$" metallocene. Since such metallocenes are not known for La and Lu, this $Ln_2(\mu\text{-}\eta^2\text{:}\eta^2\text{-}N_2)$ reduction system provides access to divalent-like reactivity with the largest and smallest diamagnetic metals in the lanthanide series. In the cyclooctatetraene reactions, changing the metal radius shows no difference in the nature of the reaction or the structure of the products. With substrates of this type, the value of using the $Ln_2(\mu\text{-}\eta^2\text{:}\eta^2\text{-}$

(47) Evans, W. J.; Seibel, C. A.; Ziller, J. W. *Inorg. Chem.* **1998**, *37*, 770.
(48) Evans, W. J.; Kozimor, S. A.; Ziller, J. W. *J. Am. Chem. Soc.* **2003**, *125*, 14264.
(49) Evans, W. J.; Davis, B. L. *Chem. Rev.* **2002**, *102*, 2119.

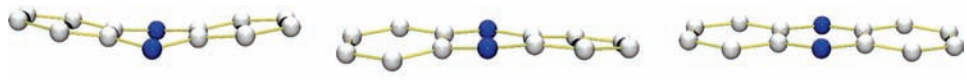

(a) (b) (c)

Figure 5. The varying degrees of planarity of the reduced phenazine dianion, $(C_{12}H_8N_2)^{2-}$ in (a) $[(C_5Me_4H)_2La](\mu\text{-}\eta^4\text{:}\eta^2\text{-}C_{12}H_8N_2)[La(THF)(C_5Me_4H)_2]$, **3**; (b) $[(C_5Me_4H)_2Lu]_2(\mu\text{-}\eta^3\text{:}\eta^3\text{-}C_{12}H_8N_2)$, **4**; and (c) $[(C_5Me_5)_2Sm]_2(\mu\text{-}\eta^3\text{:}\eta^3\text{-}C_{12}H_8N_2)$, **6**.

Table 4. Selected Bond Distances (Å) and Angles (deg) for $(C_5Me_4H)_3La(THF)$, **9**; $(C_5Me_4H)_3U(THF)$,[48] **10**; and $(C_5Me_4H)_3La$,[20] **11**

	9 (M = La)	**10** (M = U)	**11** (M = La)
Cnt−M−Cnt	116.9	116.8	120
Cnt−M−O(THF)	100.3	100.4	
M−Cnt	2.643	2.597	2.616
M−O(THF)	2.671(6)	2.650(6)	

N_2) reduction system will not depend on size optimization but simply extends analogous divalent reduction chemistry to trivalent diamagnetic complexes.

Reactions of **1** and **2** with other substrates have revealed that differences in the ionic radii of the component metals can have profound effects on reactivity. In reactions with phenazine and CO_2, complex **2** cleanly produces the expected bimetallic reduction products, $[(C_5Me_4H)_2Lu]_2(\mu\text{-}\eta^3\text{:}\eta^3\text{-}C_{12}H_8N_2)$, **4**, eq 4, and $[(C_5Me_4H)_2Lu]_2(\mu\text{-}\eta^2\text{:}\eta^2\text{-}C_2O_4)$, **5**, eq 7, respectively, while complex **1** produces complicated mixtures. In the reactions with anthracene, **2** is unreactive at room temperature, whereas **1** reacts immediately. However, only $(C_5Me_4H)_3La$[20] was isolated from the reaction mixture.

These variations show that metals of different sizes can generate different reductive reactivity results in this Ln_2N_2 system. These results also show that the reactivity is not monotonically related to metal size. This suggests that metal size is not the only factor involved in generating a high-yield reduction reaction and that the success of these reactions is highly dependent on the particular substrate.

The difference in reactivity between **1** and **2** can be rationalized by the fact that the trivalent lanthanum ion is considerably larger than that of trivalent lutetium: the nine-coordinate radii are 1.216 and 1.032 Å, respectively. In this study, the larger metal ion, La^{3+}, apparently allows for multiple reaction pathways. One reaction pathway that is clearly favored for **1** is the formation of $(C_5Me_4H)_3La$. This is supported by the fact that $(C_5Me_4H)_3La$ can be synthesized directly from $LaCl_3$ and 3 equiv of KC_5Me_4H in THF,[20] whereas the analogous Lu complex is not easily obtained via this route; it is typically made from $[(C_5Me_4H)_2Lu][(\mu\text{-}Ph)_2BPh_2]$ and KC_5Me_4H.[13]

More generally, the formation of the tris complexes, $(C_5Me_4H)_3Ln$, will be a factor that differentiates the reductive reactivity of the tetramethylcyclopentadienyl complexes, $[(C_5Me_4H)_2Ln(THF)]_2(\mu\text{-}\eta^2\text{:}\eta^2\text{-}N_2)$, from the pentamethylcyclopentadienyl analogs, $[(C_5Me_5)_2Ln(THF)]_2(\mu\text{-}\eta^2\text{:}\eta^2\text{-}N_2)$. Since $(C_5Me_5)_3Ln$ complexes do not form as readily due to steric crowding,[49] reactions that form tris(cyclopentadienyl) byproducts, for example, eqs 2 and 3, will tend to be more favorable for the $(C_5Me_4H)^-$ ligated reductants.

These reactions demonstrate the significance of developing soluble, molecular, reduction systems in which the size of the metal can be easily varied. Just as is observed in trivalent lanthanide reaction chemistry, some reduction reactions require metals of a specific optimum size to generate byproduct-free, high-yielding reactions with products that are fully characterizable by X-ray crystallography. In light of the observed differences in reductive reactivity of complexes **1** and **2**, it is remarkable how much reductive chemistry has been successful with the limited size/reduction options available in divalent lanthanide complexes. For example, it may be that the size and reduction potential of Sm^{2+} are fortuitously optimal; that is, if samarium had been either larger or smaller, it might not have led to as many new types of complexes via $(C_5Me_5)_2Sm$ and $(C_5Me_5)_2Sm(THF)_2$ reduction chemistry. On the other hand, reactions that did not provide single characterizable products with Sm^{2+} precursors may now be examined with $Ln_2(\mu\text{-}\eta^2\text{:}\eta^2\text{-}N_2)$ reductants of varying metal size.

In addition to the observed differences in the reductive reactivity of complexes **1** and **2**, size variation of the metal can also modify the coordination mode of the reduced ligand, as seen in complexes **3** and **4**. Although the small structural differences between **3** and **4** are unlikely to significantly alter the bonding or reactivity of these complexes in solution, these results demonstrate that metal size can impact the solid-state structure of complexed ions formed by reduction.

Conclusion

The accessibility of the first analogous pair of trivalent $Ln_2(\mu\text{-}\eta^2\text{:}\eta^2\text{-}N_2)$ complexes with the largest and smallest lanthanides, La^{3+} and Lu^{3+}, respectively, has provided an opportunity to evaluate the reduction chemistry of these complexes with respect to metal size. These studies have shown that with some substrates metal size effects are negligible in terms of reduction chemistry, while with other substrates the metal selection clearly makes a difference in the isolation of a single, fully characterizable reduction product. Although differences in reactivity cannot be correlated solely to metal size, it is certainly a factor that must be considered when exploring trivalent lanthanide-based reduction. The $Ln_2(\mu\text{-}\eta^2\text{:}\eta^2\text{-}N_2)$ complexes clearly can provide the equivalent of divalent "Ln^{2+}" reactivity. When diamagnetic reduction systems are desired for detailed NMR experiments, the $Ln_2(\mu\text{-}\eta^2\text{:}\eta^2\text{-}N_2)$ reduction systems have the potential to serve as substitutes for divalent reagents. This approach to lanthanide reduction is complementary to the previous types of lanthanide reduction systems because synthetic access to analogous complexes for all of the lanthanides is possible. It avoids the requirement of a divalent oxidation

state or the presence of an alkali metal. Furthermore, the byproduct of this reaction, N_2, is easily removed from the reaction mixture.

Acknowledgment. We thank the National Science Foundation for support of this research. We also thank Dr. David S. Lee for helpful discussions.

Supporting Information Available: X-ray data collection, structure solution, and refinement (PDF) and X-ray diffraction details of compounds **3**−**5** and **9** (CIF, CCDC No. 703231−703234). This material is available free of charge via the Internet at http://pubs.acs.org.

IC801853D